RESEARCH ARTICLE

Degradation of trimethoprim by sulfate radical-based advanced oxidation processes: kinetics, mechanisms, and effects of natural water matrices

Yiting Luo[1,2] · Rongkui Su[2] · Haisong Yao[2] · Aoshan Zhang[2] · Siyuan Xiang[2] · Lei Huang[3]

Abstract

In this study, we investigated the removal efficiency of a broad-spectrum antimicrobial agent trimethoprim (TMP) in a UV-activated persulfate system (UV/PS). The pseudo-first-order reaction kinetic model based on the steady-state hypothesis was used to explain TMP degradation behavior in UV-activated persulfate system. Due to the low quantum yield and molar absorptivity of TMP at 254 nm, the direct photolysis of TMP was slower. Since the free radicals generated by adding H_2O_2 or PS to the system can react with TMP, the degradation rate was significantly accelerated, and $SO_4^{\bullet-}$ played a dominant role in the UV/PS system. $k_{HO^\bullet,TMP}$ and $k_{SO_4^{\bullet-},TMP}$ were determined by the pseudo-first-order reaction kinetic model to be 6.02×10^9 and 3.88×10^9 $M^{-1}s^{-1}$, respectively. The values were consistent with competitive kinetic measurements. The pseudo-first-order reaction kinetics model can predict and explain the effect of PS concentration, natural organic matter, and chloride ion on the TMP degradation in the UV/PS system. The observed pseudo first-order rate constants for TMP degradation (k_{obs}) increased with the persulfate concentration, but it significantly decreased in the presence of NOM and chloride. SO_4^{2-} has no effect on the degradation of TMP, while HCO_3^- promotes the degradation and NO_3^- inhibits the degradation. The common transition metal ion (such as Cu^{2+}, Zn^{2+}, and Co^{2+}) in industrial wastewater has a synergistic effect on the TMP degradation in the UV/PS system, but excessive metal ions will lead to a decrease of the degradation rate.

Keywords Sulfate radical · Trimethoprim · UV/persulfate · Kinetics model

Introduction

Trimethoprim (TMP), a broad-spectrum antibacterial, has been widely used for its high effective and unique antibacterial

---

Both Yiting Luo and Rongkui Su contributed equally to this study.

Responsible Editor: Ricardo Torres-Palma

✉ Rongkui Su
surongkui@csuft.edu.cn

✉ Lei Huang
znhuanglei@foxmail.com

[1] Key Laboratory of Jiangxi Province for Persistent Pollutants Control and Resources Recycle, Nanchang Hangkong University, Nanchang 330063, PR China

[2] School of Environmental Science and Engineering, Central South University of Forestry and Technology, Changsha 410004, PR China

[3] School of Environmental Science and Engineering, Guangzhou University, Guangzhou 510006, PR China

properties. TMP can enter the environmental water through the pharmaceutical wastewater generated during industrial production processes and the domestic sewage formed during daily use. TMP concentrations up to 605 μg/L has been detected in the Pearl River basin of China (Bu et al. 2013). Residues and accumulation of TMP in the surface water and groundwater can have a major impact on the ecological environment. The priority control of 39 commonly used medicines and personal care products was studied by considering three factors: consumption, removal efficiency, and potential ecological risk, and it was found that TMP priority control ranks among the top in China (Sui et al. 2012). However, the study of Adams et al. (2002) showed that conventional water treatment processes (aluminum salt or iron salt coagulation process) cannot effectively remove TMP in surface water and deionized water. Zhao et al. (2019) used the activated sludge (AS) process to treat high-concentration antibiotic wastewater and found that the adsorption of trimethoprim was negligible, and no biodegradation occurred during the AS process.

Advanced oxidation technology (AOPs) with $^{\bullet}OH$ and $SO_4^{\bullet-}$ as the main active substance is a promising treatment technology that improves the biodegradability of wastewater through oxidation or directly degrades organic pollutants through mineralization (Hou et al. 2018; Huang et al. 2020; Ji et al. 2018). $^{\bullet}OH$ is a strong oxidant, which has a high redox potential (E_0 = 1.89~2.72 V vs. NHE). $^{\bullet}OH$ is effective in the degradation of organic pollutants. However, $\bullet OH$ has a poor selectivity, short half-life, and is easily affected by water constituents (natural organic matter, inorganic salt ions, etc.) (Wan et al. 2019). In contrast, $SO_4^{\bullet-}$ is characterized by a high redox potential (E_0 = 2.5~3.1 V vs. NHE), strong selectivity, long half-life (30~40 μs), high quantum yield, and is not easily affected by pH and organic matter (Avetta et al. 2015; Lutze et al. 2015). $SO_4^{\bullet-}$ has a good removal effect on emerging organic compounds (EOCs) (such as pharmaceuticals, disinfectants, and personal care products) in wastewater (Tang et al. 2019).

Persulfate has the characteristics of good stability and strong water solubility. Usually, under the conditions of transition metal ions (e.g., Co^{2+} and Fe^{2+}), light, heat, ultrasound, PS, or PMS can be activated to produce $SO_4^{\bullet-}$ (Ji et al. 2016; Naim and Ghauch 2016; Wei et al. 2017). UV-254nm irradiation, which has been widely used for sterilization and disinfection, is also a promising method that activates PS/PMS to generate sulfate radical efficiently (Lin et al. 2020; Zhang et al. 2021). Lin et al. (2020) studied the degradation of organosilicon wastewater by UV-based advanced oxidation processes: UV/H₂O₂, UV/peroxydisulfate (PDS), and UV/peroxymonosulfate (PMS), and the results showed that UV/PDS achieved a higher COD removal (90.6%) than UV/PMS (80.8%) after a 240 min reaction time. Ran and Li (2020) studied refractory organic compounds from dinitrodiazophenol (DDNP) containing industrial wastewater degraded through two ultraviolet (UV)-based advanced oxidation processes: UV/hydrogen peroxide (UV/H₂O₂) and UV/potassium persulfate (UV/PS) processes, and the results showed that the UV/PS process exhibited a higher organic compound removal efficiency and better applicability. Bougdour et al. (2020) studied the removal efficiency of colors from wastewater containing mixed primary direct dyes and real textile industry wastewater using PDS (peroxydisulfate)/Fe(II)/UV process, and it was found that PDS/Fe(II)/UV is the best treatment method for real textile wastewater. Zhang et al. (2015) studied the degradation of drugs and metabolites in synthetic human urine by UV, UV/H₂O₂, and UV/PMS (pH = 6 and pH = 9), respectively. The results showed that UV/H₂O₂ and UV/PMS had a better degradation effect on TMP. However, the degradation of TMP by UV/PS system under neutral condition has not been reported yet. The effects of complex environmental matrices and transition metal ions present in industrial wastewater on the degradation of TMP by UV/PS are unclear.

This study aims to establish an efficient UV/PS technology to degrade EOCs in wastewater. TMP is used as the target compound. Under the steady-state assumption, the pseudo-first-order reaction kinetic model is used to study the degradation mechanism of TMP in a UV/PS system. Competitive kinetics technique and kinetics model were used to determine $k_{TMP,SO_4^{\bullet-}}$. The effects of persulfate concentration and matrix components (natural organic matters, inorganic anions) were evaluated by the kinetics model and experiment. Then, the effects of transition metal ions (Cu^{2+}, Zn^{2+}, Co^{2+}) in industrial wastewater on the photodegradation kinetics of TMP were further evaluated.

Experimental method

Materials

TMP (99.0%), 4-chlorobenzoic acid (*p*CBA, 99.0%), sodium dihydrogen phosphate (99.0%), disodium phosphate (99.0%), sodium persulfate (99.0%), fulvic acid (technical), and *t*-butanol (99.7%) were obtained from Sigma Aldrich. Copper sulfate (guaranteed reagent, GR), cobalt sulfate (GR), zinc sulfate (GR), sodium chloride (GR), sodium sulfate (analytical grade), sulfuric acid (GR), and hydrogen peroxide (30% by weight) were obtained from Sinopharm Chemical Reagent. Deionized (DI) water was obtained from a Molresearc 1010A molecular water system.

Irradiation experiments

In the kinetics tests, the initial concentrations of the target compound TMP and probe compound *p*CBA are both set at 10 uM. Phosphate buffer system (NaH₂PO₄/Na₂HPO₄, 10mM) was used to stabilize solution pH at 7.55. The value of pH did not change during the experiments. The detailed experimental design, operation process, data collection, and result analysis had been described in our previous articles (Su et al. 2018; Yang et al. 2017).

Analytical methods

According to the measurement method we previously reported, the average light intensity per volume (I_0) and effective optical path length (*b*) were determined to be 7.496×10^{-6} Einstein L^{-1} s^{-1} and 0.935 cm, respectively (Beltran et al. 1995; Parker 1953; Yang et al. 2017).

A USB 2000+, Ocean Optics fiber optic spectrometer was used to measure the emission spectrum and light intensity of low-pressure mercury lamp. Shimadzu UV-1800 spectrometer was used to determine the absorption spectra of TMP and

*p*CBA (Fig. 1). A Mettler Toledo S220 pH meter was used to measure the solution pH.

The concentration of TMP and *p*CBA was performed using an ultra-performance liquid chromatography (Waters ACQUITY H-Class) with a BEH C18 column (1.7 μm, 2.1 mm × 50 mm, Waters). The detailed method is shown in Table 1.

Results and discussion

Degradation of TMP in UV, UV/H$_2$O$_2$, and UV/PS systems

Linear regression analysis of the TMP degradation process showed that it followed the pseudo-first-order reaction kinetics. As shown in Fig. 2, under the reaction conditions of UV intensity 7.496×10^{-6} Einstein L -1 s -1, pH = 7.55, and [TMP]$_0$ = 10 μM, the initial direct photolytic degradation rate of TMP in only the UV system was 0.038 μM min -1. Without UV irradiation, the dark reaction experiments showed that TMP had no degradation. The same results were observed in the presence of H$_2$O$_2$ or PS. Therefore, the degradation of TMP under UV radiation was mainly attributed to the direct photolysis of TMP. As shown in Fig. 1, at the wavelength ranging from 250 to 260 nm, TMP has a relative trough in the absorption of light. Therefore, the direct photolysis of TMP under 254 nm ultraviolet mercury lamp irradiation is slower.

The molar absorption coefficient (ε) and quantum yield (φ) are two important factors that affect the kinetics of target compound direct photolysis (Pereira et al. 2007). The molar absorption coefficient is a measure of the absorb light ability of a target compound at a specific wavelength (λ). ε can be calculated as Eq. 1.

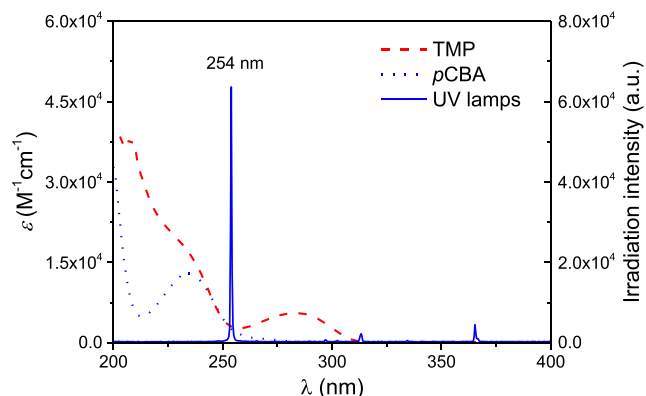$$A = \varepsilon_{TMP} \times [TMP] \times l \tag{1}$$

Fig. 1 Decadic molar absorption coefficient (ε) of TMP and *p*CBA (pH = 7.55) with reference to the UV lamp emission spectra from 200 to 400 nm

A is the absorbance of 10 μM TMP solutions. The TMP solution pH is adjusted to 7.55 by phosphate buffer solution. *l* is the path length of quartz cuvette. In this study, a 1 cm path length quartz cuvette was used to measure the TMP solution absorbance. Figure 1 illustrates the decadic molar extinction coefficient for TMP with reference to Hg lamp emission spectra. At the wavelength of 254 nm, the ε values of TMP were 3078.56 M^{-1} cm^{-1}, which is consistent with the reported value of 2942 M^{-1} cm^{-1} (Baeza and Knappe 2011). ε_{TMP} was lower than the reported value of carbamazepine (6070 M^{-1} cm^{-1}) and sulfamethoxazole (16580 M^{-1} cm^{-1}), while it was higher than that of ibuprofen (256 M^{-1} cm^{-1}) and bisphenol (750 M^{-1} cm^{-1}) (Baeza and Knappe 2011; Pereira et al. 2007; Yuan et al. 2009).

The quantum yield described the ratio of the total numbers of molecules of the compound destroyed to the total numbers of photons absorbed by the system. The quantum yield of TMP can be calculated as follows (Pereira et al. 2007):

$$\varphi_{TMP} = \frac{r_{UV}}{I_0 \times \left(1 - 10^{-\varepsilon_{TMP} \, b \, [TMP]}\right)} \tag{2}$$

where φ_{TMP} is the quantum yield of TMP at 254 nm (mol Einstein^{-1}), r_{uv} (M s^{-1}) is the direct photolytic degradation rate at an initial concentration of 10 μM. I_0 is the incident UV intensity, ε_{TMP} is the molar extinction coefficient of TMP at wavelength 254 nm, and b is the reactor light path. φ_{TMP} was calculated to be 1.29×10^{-3} mol Einstein^{-1}, which was close to the reported value of 1.18×10^{-3} M^{-1} cm^{-1} (Baeza and Knappe 2011). Different Pharmaceutical and Personal Care Products (PPCPs) have different molecular structures, which can result in different quantum yield values (Yuan et al. 2009). The value of φ_{TMP} was relatively low compared to the values of other PPCPs (ibuprofen, 0.192 M^{-1} cm^{-1} and sulfamethoxazole, 0.0215 M^{-1} cm^{-1}) (Yang et al. 2016; Yuan et al. 2009).

Due to the relatively low molar absorptivity and extremely low quantum yield, the direct photolysis degradation rate of TMP was slow. As shown in Fig. 2, the degradation kinetics of TMP was significantly enhanced by adding 100 μM H$_2$O$_2$/ PS compared to direct photolysis. The initial degradation rate in the UV/H$_2$O$_2$ and UV/PS systems was 1.657 μM min^{-1} and 2.581 μM min^{-1}, respectively. These results indicated that the degradation of TMP in the UV/H$_2$O$_2$ or UV/PS systems included direct photolysis and radical degradation, but radical degradation played a major role (more than 95%). The enhanced degradation of TMP with the addition of H$_2$O$_2$ or PS was due to the fact that TMP degradation mainly contributed to $^{\bullet}$OH/SO$_4^{\bullet-}$ radical-mediated oxidation. The results were consistent with the results reported by Kwon et al. (2015), and they also demonstrated that $^{\bullet}$OH/SO$_4^{\bullet-}$ played a major role in the degradation of ibuprofen by UV/H$_2$O$_2$ or UV/PS.

Table 1 The detailed method of measure the concentration of TMP and pCBA

Compound	Acetonitrile	Phosphate buffer (20 mM and pH 3)	λ nm	Flow rate mL min^{-1}	Injection volume μl	Column temperature °C
TMP	15%	85%	285	0.3	5	35
pCBA	30%	70%	238			

Therefore, the degradation rate constants of TMP largely depended on the formation of $^{\bullet}OH/SO_4^{\bullet-}$ in the UV system.

The competitive kinetics method was used to determine the second-order rate constants of TMP with $SO_4^{\bullet-}$ ($k_{SO_4^{\bullet-},TMP}$), and pCBA ($k_{SO_4^{\bullet-},pCBA} = 3.60 \times 10^8$ M^{-1} s^{-1}) was chosen as a reference compound in this study (Kwon et al. 2015). The 1 mM t-butanol was added to suppress any contribution of $^{\bullet}OH$ in oxidizing TMP. The competitive kinetics method had been described in detail in our previous study (Yang et al. 2017). Figure 3 shows that an average reaction rate constant ratio between TMP and pCBA with $SO_4^{\bullet-}$ was 10.58. The $k_{SO_4^{\bullet-},TMP}$ values were determined to be 3.81×10^9 M^{-1} s^{-1}. It was lower than the reported value of 7.71×10^9 M^{-1} s^{-1} (Zhang et al. 2015). pH values determine the morphology of TMP in the system. The possible reason was that our pH conditions (pH = 7.55) are different from those of Zhang (pH = 6).

Pseudo first-order reaction kinetics

The steady-state approximation for the kinetic description of radicals was also used to estimate the $k_{SO_4^{\bullet-},IBU}$ (Luo et al. 2016a; Yang et al. 2017). The model was developed based on the hypothesis that the degradation of the target compound depended primarily on radicals (i.e., $SO_4^{\bullet-}$ and $^{\bul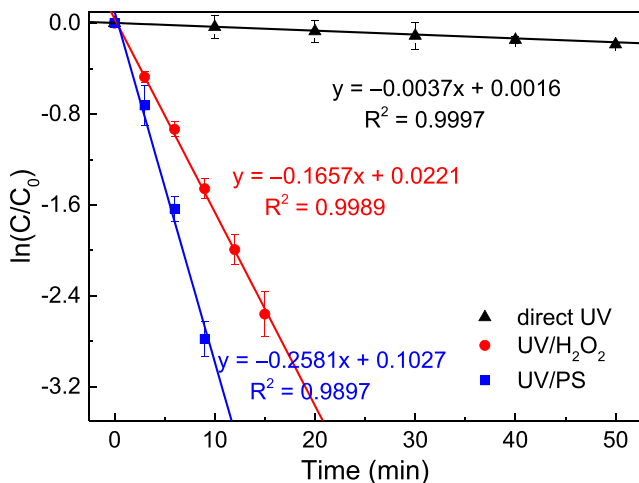let}OH$) generated from the irradiation of PS. $SO_4^{\bullet-}$ was produced from activation of $S_2O_8^{2-}$ by UV and $^{\bullet}OH$ was simultaneously formed from the reaction of $SO_4^{\bullet-}$ with H_2O or OH^-. The reactions in the UV/PS system and these second-order rate constants are presented in Table 2.

Under steady-state conditions, $k_{SO_4^{\bullet-},TMP}$, $[SO_4^{\bullet-}]_{SS}$ and $[HO^{\bullet}]_{SS}$ can be expressed (for detailed derivation process, see previous paper, Yang et al. 2017):

$$k_{SO_4^{\bullet-},TMP} = \frac{r_{0,SO_4^{\bullet-}}\, k_{HO^{\bullet},TMP}\, \alpha - \beta(k_{app} - k_{UV})}{(k_{app} - k_{UV})[TMP] - r_{0,SO_4^{\bullet-}}} \quad (3)$$

$$[SO_4^{\bullet-}]_{SS} = \frac{(k_{app} - k_{UV})[TMP] - r_{0,SO_4^{\bullet-}}}{\alpha\, k_{HO^{\bullet},TMP}[TMP] - \beta} \quad (4)$$

$$[HO^{\bullet}]_{SS} = \frac{\alpha\left((k_{app} - k_{UV})[TMP] - r_{0,SO_4^{\bullet-}}\right)}{\alpha k_{HO^{\bullet},TMP}[TMP] - \beta} \quad (5)$$

$$\alpha = \frac{k_2[OH^-] + k_3[H_2O]}{k_{HO^{\bullet},TMP}[TMP] + k_7[S_2O_8^{2-}] + k_{11}[H_2PO_4^-] + k_{12}[HPO_4^{2-}]} \quad (6)$$

$$\beta = k_2[OH^-] + k_3[H_2O] + k_4[S_2O_8^{2-}] + k_9[H_2PO_4^-] + k_{10}[HPO_4^{2-}] \quad (7)$$

The average of $r_{0\_SO_4^{\bullet-}}$ and k_{app} was 4.623×10^{-8} M s^{-1} and 4.301×10^{-3} s^{-1}, respectively. The value of α was 8.78×10^{-3} (unitless), and β was 9.00×10^3 s^{-1} as calculated. $k_{HO^{\bullet},TMP}$ was

Fig. 2 Time-dependent degradation kinetics of TMP in the UV, UV/H$_2$O$_2$, and UV/PS systems ([TMP]$_0$ = 10 μM, [H$_2$O$_2$] = [PS] = 100 μM, pH = 7.55, and I_0 = 7.496×10^{-6} Einstein L^{-1} s^{-1}). The degradation was fit to a pseudo first-order kinetic model (lines)

In Fig. 2:
y = −0.0037x + 0.0016, R^2 = 0.9997
y = −0.1657x + 0.0221, R^2 = 0.9989
y = −0.2581x + 0.1027, R^2 = 0.9897
▲ direct UV
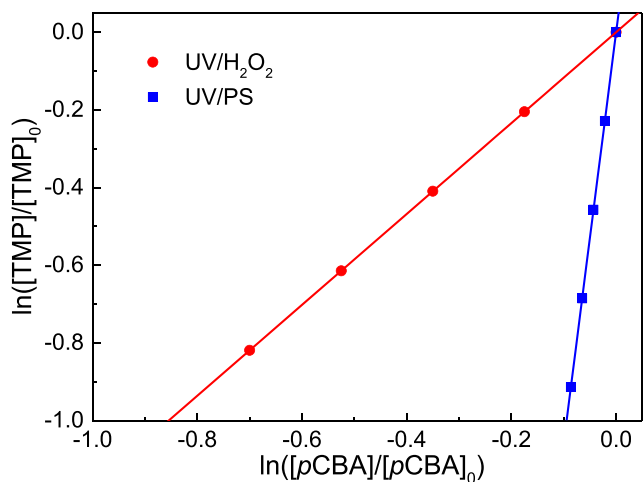● UV/H$_2$O$_2$
■ UV/PS

Fig. 3 Competitive oxidation of TMP and pCBA in UV/H$_2$O$_2$ and UV/PS system

Table 2 Summary of the reactions in the UV/PS system (pH = 7.55 and 10 mM phosphate buffer)

#	Reaction	k (M^{-1} s^{-1}, unless specified)	Reference or note
1	$S_2O_8^{2-} + h\nu \rightarrow 2SO_4^{\bullet-}$	$r_{0,SO_4^{\bullet-}} = 2\varphi_S E_S$, M s^{-1}	Measured in this study
2	$SO_4^{\bullet-} + OH^- \rightarrow SO_4^{2-} + {}^\bullet OH$	$k_2 = 6.5 \times 10^7$	(Neta et al. 1977)
3	$SO_4^{\bullet-} + H_2O \rightarrow HSO_4^- + {}^\bullet OH$	$k_3 = 8.3$	(Yu et al. 2004)
4	$SO_4^{\bullet-} + S_2O_8^{2-} \rightarrow S_2O_8^{\bullet-} + SO_4^{2-}$	$k_4 = 5.5 \times 10^5$	(Yu et al. 2004)
5	$SO_4^{\bullet-} + SO_4^{\bullet-} \rightarrow S_2O_8^{2-}$	$k_5 = 4.4 \times 10^8$	(Klaning et al. 1991)
6	$SO_4^{\bullet-} + {}^\bullet OH \rightarrow H^+ + SO_4^{2-} + O_2$	$k_6 = 9.5 \times 10^9$	(Klaning et al. 1991)
7	${}^\bullet OH + S_2O_8^{2-} \rightarrow S_2O_8^{\bullet-} + OH^-$	$k_7 = 1.4 \times 10^7$	(Buxton et al. 1988)
8	${}^\bullet OH + {}^\bullet OH \rightarrow H_2O_2$	$k_8 = 5.5 \times 10^9$	(Buxton et al. 1988)
9	$H_3PO_4 \rightleftharpoons H^+ + H_2PO_4^-$	$pK_{a1} = 2.1$ unitless	(Stumm and Morgan 1996)
10	$H_2PO_4^- \rightleftharpoons H^+ + HPO_4^{2-}$	$pK_{a2} = 7.2$ unitless	(Stumm and Morgan 1996)
11	$HPO_4^{2-} \rightleftharpoons H^+ + PO_4^{3-}$	$pK_{a3} = 12.3$ unitless	(Stumm and Morgan 1996)
12	$SO_4^{\bullet-} + H2PO_4^- \rightarrow products$	$k_9 < 7.2 \times 10^4$	(Neta et al. 1977)
13	$SO_4^{\bullet-} + H2PO_4^{2-} \rightarrow products$	$k_{10} = 1.2 \times 10^6$	(Neta et al. 1977)
14	${}^\bullet OH + H2PO_4^- \rightarrow HPO_4^{\bullet-} + H2O$	$k_{11} = 2.0 \times 10^4$	(Buxton et al. 1988)
15	${}^\bullet OH + HPO_4^{2-} \rightarrow HPO_4^{\bullet-} + OH^-$	$k_{12} = 1.5 \times 10^5$	(Buxton et al. 1988)
	In the presence of *p*CBA and *t*-butanol		
16	$SO_4^{\bullet-} + t-butanol \rightarrow products$	$k_{13} = 4.0 \times 10^5$	(Neta et al. 1977)
17	${}^\bullet OH + t-butanol \rightarrow products$	$k_{14} = 6.0 \times 10^8$	(Buxton et al. 1988)
18	$SO_4^{\bullet-} + pCBA \rightarrow products$	$k_{15} = 3.6 \times 10^8$	(Fang and Shang 2012)
19	${}^\bullet OH + pCBA \rightarrow products$	$k_{16} = 5.0 \times 10^9$	(Fang and Shang 2012)
	In the presence of HA		
20	$SO_4^{\bullet-} + FA \rightarrow products$	$k_{17} = 9.3 \times 10^3$ L mgC^{-1} s^{-1}	measured in this study
21	${}^\bullet OH + FA \rightarrow products$	$k_{18} = 1.4 \times 10^4$ L mgC^{-1} s^{-1}	(Lutze et al. 2015)
	In the presence of Cl⁻		
22	$SO_4^{\bullet-} + Cl^- \rightarrow Cl^\bullet + SO_4^{2-}$	$k_{19} = 3.0 \times 10^8$	(Das 2001)
23	${}^\bullet OH + Cl^- \rightarrow ClOH^\bullet$	$k_{20} = 4.3 \times 10^9$	(Jayson et al. 1973)
24	$Cl^\bullet + OH^- \rightarrow ClOH^\bullet$	$k_{21} = 1.8 \times 10^{10}$	(Kläning and Wolff 1985)
25	$Cl^\bullet + H_2O \rightarrow ClOH^\bullet + H^+$	$k_{22} = 2.5 \times 10^5$	(Jayson et al. 1973)
26	$ClOH^\bullet \rightarrow Cl^- + {}^\bullet OH$	$k_{23} = 6.0 \times 10^9$	(Jayson et al. 1973)
27	$ClOH^\bullet + H^+ \rightarrow Cl^\bullet + H_2O$	$k_{24} = 2.1 \times 10^{10}$	(Kläning and Wolff 1985)
28	$Cl^\bullet + Cl^- \rightarrow Cl_2^{\bullet-}$	$k_{25} = 8.5 \times 10^9$	(Yu et al. 2004)
29	$Cl_2^{\bullet-} + H_2O \rightarrow HClOH + Cl^-$	$k_{26} = 1.3 \times 10^3$	(McElroy 1990)
30	$Cl_2^{\bullet-} + OH^- \rightarrow ClOH^{\bullet-} + Cl^-$	$k_{27} = 4.5 \times 10^7$	(Kläning and Wolff 1985)
31	$Cl_2^{\bullet-} + Cl_2^{\bullet-} \rightarrow Cl_2 + 2Cl^-$	$k_{28} = 9.0 \times 10^8$	(Yu et al. 2004)
32	$Cl_2^{\bullet-} + Cl^\bullet \rightarrow Cl_2 + Cl^-$	$k_{29} = 2.1 \times 10^9$	(Nikravesh et al. 2020)
	Degradation of TMP		
33	$TMP + h\nu \rightarrow products$	r_{uv}, M s^{-1}	Measured in this study
34	${}^\bullet OH + TMP \rightarrow products$	$k_{TMP,HO^\bullet}$	measured in this study
35	$SO_4^{\bullet-} + TMP \rightarrow products$	$k_{TMP,SO_4^{\bullet-}}$	measured in this study

Note: In phosphate buffer, $H2PO_4^-$ and HPO_4^{2-} are the predominant species at pH 7.55

$6.02 \pm 0.13 \times 10^9$ $M^{-1}s^{-1}$ from competition kinetics method in this study. $k_{SO_4^{\bullet-},TMP}$ was determined to be $3.88 \pm 0.07 \times 10^9$ M^{-1} s^{-1}, which was consistent with the value determined by competitive kinetics. The average of $\left[SO_4^{\bullet-}\right]_{SS}$ and $[HO^\bullet]_{SS}$ was 9.46×10^{-15} M and 1.08×10^{-12} M, respectively.

With the values of $k_{HO^\bullet,TMP}$, $k_{SO_4^{\bullet-},TMP}$, $[HO^\bullet]_{SS}$, $\left[SO_4^{\bullet-}\right]_{SS}$, the contribution of direct UV photolysis, ${}^\bullet OH$, and $SO_4^{\bullet-}$ in degrading TMP was calculated. In the UV/PS system, the values of r_{uv}, $r_{HO^\bullet}$, and $r_{SO_4^{\bullet-}}$ were determined to be 6.22×10^{-10} M s^{-1}, 5.69×10^{-10} M s^{-1}, and 4.18×10^{-8} M s^{-1},

respectively. Thus, approximately 1.45% of TMP removal was attributed to direct photolysis and $^{\bullet}$OH only contributed to about 1.32% of the total degradation, indicating that $SO_4^{\bullet-}$ played a dominant role during the degradation process.

The pseudo first-order reaction kinetics model can be used to study and simulate the effects of other factors on TMP degradation. In this study, we used the pseudo first-order reaction kinetics model to predict and explain the effects of PS concentration and matrix components on TMP degradation by UV/PS process. Then the contributions of $^{\bullet}$OH and $SO_4^{\bullet-}$ to TMP degradation (i.e., $k_{cal,\ UV}$, $k_{cal,\ \bullet OH}$ and k_{cal,SO_4^-}) under various experimental conditions were calculated by Eqs. 8, 9, and 10, respectively.

$$k_{cal,UV} = \varphi_{TMP} \times E_0 \times \frac{b\,\varepsilon_{TMP}}{A} \times \left(1 - e^{-2.303A}\right) \tag{8}$$

$$k_{cal,HO^{\bullet}} = k_{TMP,HO^{\bullet}} \times [HO^{\bullet}]_{SS} \tag{9}$$

$$k_{cal,SO_4^-} = k_{TMP,SO_4^-} \times \left[SO_4^{\bullet-}\right]_{SS} \tag{10}$$

The total contribution of $^{\bullet}$OH and $SO_4^{\bullet-}$ to TMP degradation (k_{cal}) can be expressed by Eq. 11.

$$k_{cal} = k_{cal,UV} + k_{cal,HO^{\bullet}} + k_{cal,SO_4^-} \tag{11}$$

Effect of the initial oxidant concentration

The degradation rates of TMP were affected by the PS concentration in the UV/PS system. As shown in Fig. 4, the observed pseudo first-order rate constants (in the unit of s^{-1}) for TMP degradation (k_{obs}) increased from 4.95×10^{-3} s^{-1} to 25.12×10^{-3} s^{-1} when PS concentration increases from 100 μM to 500 μM. This result could be accurately predicted by the kinetic model (the calculated result, k_{cal}). The contributions of direct UV, $^{\bullet}$OH, and $SO_4^{\bullet-}$ to TMP degradation were
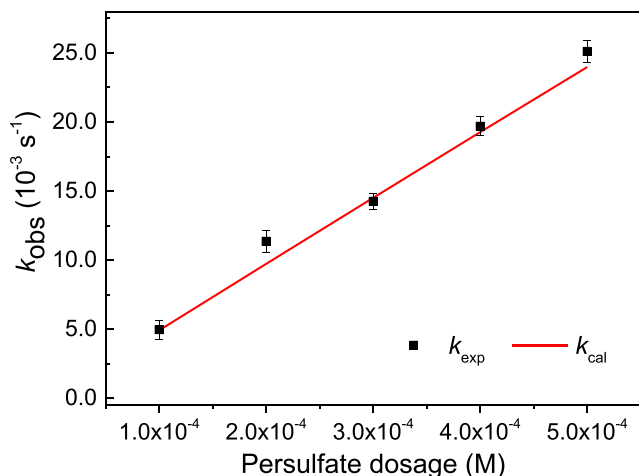

Fig. 4 Impacts of PS concentration on the pseudo first-order constants of TMP (k). ([TMP]$_0$ = 10 μM, pH = 7.55, and $I_0 = 7.496 \times 10^{-6}$ Einstein L^{-1} s^{-1})

also calculated. As the dose of PS increased, the contribution rate of direct photolysis was significantly reduced due to the competition of PS for UV, and there was no significant change in the contribution rate of $^{\bullet}$OH. However, the results showed that $SO_4^{\bullet-}$ was the main reactive species in the UV/PS system at pH 7.55, with a contribution to TMP degradation (k_{cal,SO_4^-}) always greater than 97%. This result was also consistent with the previous study of Luo et al. (2016a) who found that the contribution of $SO_4^{\bullet-}$ was increased from 82.6 to 92.5% with the increase of PS concentration from 100 to 500 μM in the degradation of 2,4,6-trichloroanisole. However, Xie et al. (2015) found that the contribution of $^{\bullet}$OH was about 3.5 times and 2.0 times higher than $SO_4^{\bullet-}$ for 2-methylisoborneol and geosmin degradation, respectively. This discrepancy might be ascribed to the secondary reaction rate constant of radicals with the target compound and the concentration of free radicals in the system. The $k_{\bullet OH}/k_{SO_4^-}$ of 2,4,6-trichloroanisole and TMP were 1.37 and 1.55, which is smaller than the value of 2-methylisoborneol and geosmin (10.24 and 7.50, respectively). On the other hand, $\left[SO_4^{\bullet-}\right]_{SS}$ was expected to be about two orders of magnitude higher than $[HO^{\bullet}]_{SS}$ based on Eqs. 4 and 5, which was consistent with Luo's study (Luo et al. 2016a). For instance, the calculated steady-state concentrations of $SO_4^{\bullet-}$ and $^{\bullet}$OH were about 1.08×10^{-12} M and 9.46×10^{-15} M at [PS] = 100 μM, respectively.

Effect of NOM

NOM is a mixture of macromolecular organic compounds prevalent in the natural environment, widely distributed in soil, lake, river, and ocean. The impact of NOM on the degradation of organic contaminants has received more and more attention. Fulvic acid (FA) is a mixture of non-homogeneous compounds that can be dissolved in a base but cannot be dissolved in acid (Fu et al. 2006). Since FA was the main component of NOM, the effect of NOM in the UV/PS processes was examined by adding different concentrations of FA (0~2.88 mgC L^{-1}) in this study. Figure 5 shows that k_{obs} decreased from 11.36×10^{-3} s^{-1} to 7.07×10^{-3} s^{-1} with FA concentrations increasing from 0 to 2.88 mgC L^{-1}. The experimental data was basically consistent with the modeling results (k_{cal}). Two factors could be responsible for the inhibitory effect of FA on TMP degradation. First, FA would exert an inner filter effect for the photolysis of persulfate, and A can be modified to $A = b(\varepsilon_{TMP}[TMP] + \varepsilon_{S_2O_8^{2-}} [S_2O_8^{2-}] + \varepsilon_{FA}[FA])$ ($\varepsilon_{FA} = 0.10$ L mgC^{-1} cm^{-1} measured in this work). Second, FA acted as a radical scavenger as described by Eqs. 20 and 21 in Table 2. The kinetic model was used to estimate the relative contributions of the inner filter effect and radical scavenger in decreasing k_{obs} values. If the inner filter effect of FA was not accounted for k, then ε_{FA} was equal to zero. As we can see from Fig. 5, k_{cal} (green line) slightly changed as compared to
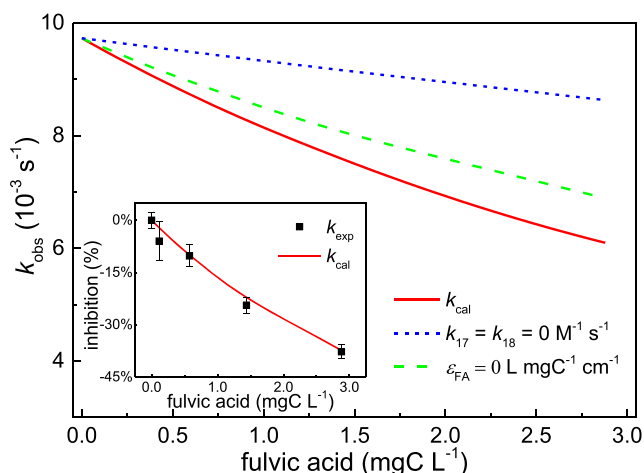
Fig. 5 Impacts of fulvic acid on the pseudo first-order constants of TMP (k) ([TMP]$_0$ = 10 μM, [PS]$_0$ = 200 μM, pH = 7.55, and E_0 = 7.496×10^{-6} Einstein L^{-1} s^{-1})

the experimental data (black dots) by assuming $\varepsilon_{FA} = 0$. If FA did not have a radical scavenging effect (i.e., k_{17} and k_{18} values in Table 2 were equal to zero), k_{cal} (blue line) greatly deviated from the experimental data (black dots) in Fig. 5. These results indicated that the radical scavenger effect of FA played a more significant role than the inner filter effect in decreasing TMP degradation rates. At the same time, the model calculation results showed that as the concentration of fulvic acid increased, the contribution rate of direct photolysis and SO$_4^{\bullet-}$ to TMP degradation did not change significantly, and the contribution rate of $^{\bullet}$OH dropped significantly. The possible reason was that $k_{FA, \bullet OH}$ (3.0×10^8 M$_C^{-1}$s^{-1}) was larger than $k_{FA, SO_4^{\bullet-}}$ (2.35×10^7 M$_C^{-1}$s^{-1}) (Weishaar et al. 2003; Xie et al. 2015).

Effect of inorganic anions

Inorganic anions present in environmental water (e.g., SO$_4^{2-}$, NO$_3^-$, Cl$^-$, and HCO$_3^-$) also have a greater effect on the degradation of TMP by UV/PS. In this study, the effect of inorganic ions on the degradation kinetics of SO$_4^{\bullet-}$ was studied by adding anion concentrations close to those in the environment in deionized water (SO$_4^{2-}$ and NO$_3^-$ concentration of 0.5 mM, Cl$^-$ and HCO$_3^-$ the concentration is 1 mM). The results (Fig. 6) show that SO$_4^{2-}$ has little effect on the degradation of TMP, while HCO$_3^-$ will promote the degradation of TMP (11.5%). The main reason why HCO$_3^-$ promotes the TMP degradation in the UV/PS system is that HCO$_3^-$ can react with SO$_4^{\bullet-}$ to produce CO$_3^{\bullet-}$ (1.59 V NHE), which has certain oxidation ability. The oxidation potential of CO$_3^{\bullet-}$ was 1.59 V vs NHE (Giannakis et al. 2021). The secondary free radicals CO$_3^{\bullet-}$ can continue to react with TMP (Lian et al. 2017; Luo et al. 2016b; Zuo et al. 1999). NO$_3^-$ and Cl$^-$ will inhibit the degradation of TMP, and the inhibition rates are 32.1% and

20.4%, respectively. NO$_3^-$ can produce $^{\bullet}$OH, NO$_3^{\bullet-}$, and NO$_2^{\bullet-}$ under a series of complex reactions under UV and sunlight (Dong and Rosario-Ortiz 2012; Ji et al. 2012; Keen et al. 2012; Vione et al. 2006; Xiao et al. 2014). The oxidation potentials of NO$_3^{\bullet-}$ and NO$_2^{\bullet-}$ were 2.3–2.5 V and 1.03 V, respectively (Giannakis et al. 2021). However, $^{\bullet}$OH, NO$_2^{\bullet-}$, and NO$_2^-$ have lower quantum yields, $\Phi_{\bullet OH/NO_2^-}$ =0.24, $\Phi_{NO_2^-}$ =0.015~0.028 mol Einstein^{-1} (Keen et al. 2012). According to Keen's calculation, the [HO$^{\bullet}$]$_{SS}$ produced by UV excitation 0.5 mM NO$_3^-$ is only 0.74×10^{-18} M (Keen et al. 2012). At the same time, NO$_3^-$ can also quench $^{\bullet}$OH/ SO$_4^{\bullet-}$. In the UV/S$_2$O$_8^{2-}$ system, Cl$^-$ and SO$_4^{\bullet-}$ can react to produce a series of new secondary free radicals, such as Cl$^{\bullet}$, ClOH$^{\bullet-}$, and Cl$_2^{\bullet-}$ (Luo et al. 2016b). The oxidation potentials of Cl$^{\bullet}$, ClOH$^{\bullet-}$ and Cl$_2^{\bullet-}$ were 1.9V, 2.47 V, and 2.0 V, respectively (Giannakis et al. 2021). On the one hand, Cl$^-$ can quench SO$_4^{\bullet-}$ (Lian et al. 2017; Yang et al. 2014; Yang et al. 2016). On the other hand, the generated secondary free radicals can continue to oxidatively degrade TMP. Cl$^{\bullet}$ and Cl$_2^{\bullet-}$ have strong oxidation ability. The oxidation potentials of Cl$^{\bullet}$ and Cl$_2^{\bullet-}$ were 2.47 V and 2.0 V, respectively (Beitz et al. 1998). Cl$^{\bullet}$ is also a selective oxidant, which can react with electron-rich components through electron transfer, hydrogen extraction, and addition (Beitz et al. 1998). Therefore, the contribution of secondary free radicals (Cl$^{\bullet}$, ClOH$^{\bullet-}$, and Cl$_2^{\bullet-}$) and the inhibition of Cl$^-$ comprehensive determine the effect on TMP degradation.

The effect of Cl$^-$ on TMP degradation was studied using concentrations ranging from 0 to 5 mM. As shown in Fig. 7, for the effect of Cl$^-$, k_{obs} slightly decreased from 11.36×10^{-3} s^{-1} in the absence of Cl$^-$ to 5.73×10^{-3} s^{-1} in the presence of 5 mM Cl$^-$. The negative effect of Cl$^-$ in the system might result from the fact that significant amounts of SO$_4^{\bullet-}$ react with Cl$^-$ forming chloride-derived radicals. For instance, the influence of Cl$^-$ depended on its fast rate constants with both $^{\bullet}$OH and SO$_4^{\bullet-}$ (Eqs. 22 and 23 in Table 2). Usually, the fast
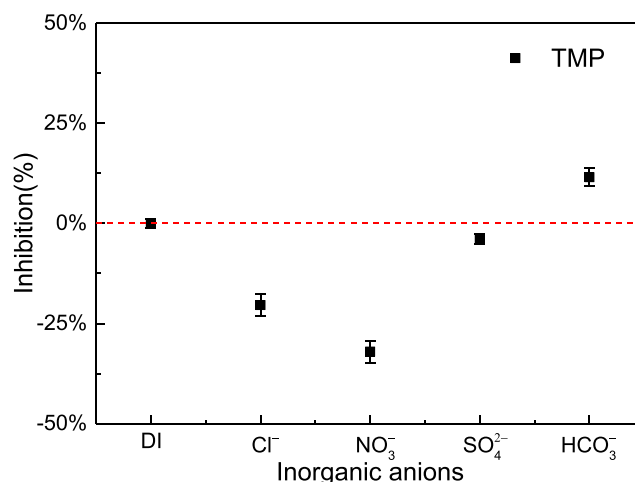

Fig. 6 Inhibition of inorganic anions on TMP degradation in DI water

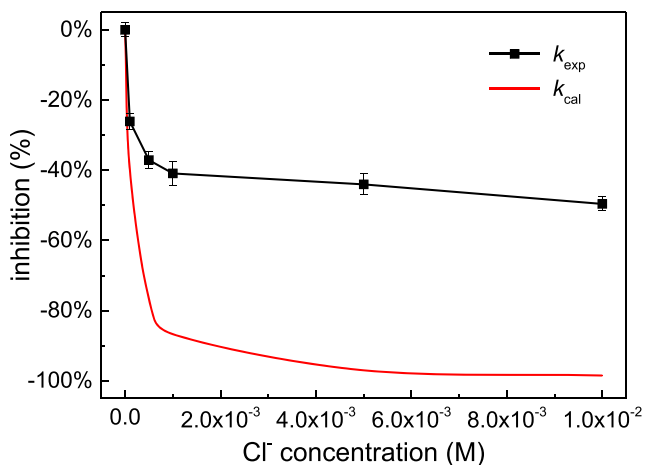**Fig. 7** Impacts of Cl⁻ on the degradation of TMP ($[TMP]_0 = 10$ μM, $[PS]_0 = 200$ μM, pH = 7.55, and $E_0 = 7.496 \times 10^{-6}$ Einstein L^{-1} s^{-1})

reaction of $SO_4^{\bullet-}$ with Cl⁻ yields secondary reactive chlorine radical species, such as $Cl^{\bullet}$, $ClOH^{\bullet}$, and $Cl_2^{\bullet-}$ through complex chain reactions (i.e., Eqs. 24 to 31 in Table 2).

Since most of those rate constants of reactive chlorine radicals with TMP are relatively unknown, it is difficult to accurately predict how Cl⁻ affected TMP degradation in the UV/PS process by the steady-state kinetic model. Thus, in this study, only Cl⁻ was considered the scavenger of $^{\bullet}OH$ and $SO_4^{\bullet-}$ for calculating the k_{cal} values. As shown in Fig. 6, k_{cal} was significantly smaller than the experimental data (red line), which contradicts the observation that Cl⁻ had a minor inhibitory effect on TMP degradation. Still, those secondary radicals might play a role in the degradation of TMP in UV/PS process, since $Cl^{\bullet}$ and $Cl_2^{\bullet-}$ were strong oxidants with oxidation potentials of 2.47 V and 2.0 V, respectively (Beitz et al. 1998). $Cl^{\bullet}$ is a selective oxidant that reacts with electron-rich moieties through one-electron oxidation, H-abstraction, and addition to unsaturated bonds (Grebel et al. 2010). Previous studies had shown conflicting results of Cl⁻ in the $UV/S_2O_8^{2-}$ process, depending on the target compound. Yuan et al. (2011) reported that a dual effect of chloride (i.e., inhibitory and accelerating effect) on azo dye (Acid Orange 7) degradation in an emerging cobalt/peroxymonosulfate (Co/PMS) advanced oxidation process. Ghauch et al. (2017) showed that the k value of chloramphenicol increased first and then decreased with the concentration increase of chloride anion in UV/PS system. The reaction between $^{\bullet}OH/SO_4^{\bullet-}$ and Cl⁻ produces secondary chlorine radical species, but the influence of Cl⁻ was compound dependent, either promoting target compound removal (Criquet and Leitner 2009; Fang et al. 2012), or inhibiting the degradation (Liang et al. 2006; Shah et al. 2013).
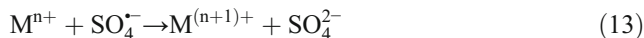
Effect of transition metal ions

Transition metal ions (M^{n+}) were very common in industrial wastewater, and some research results showed that the

presence of M^{n+} had a very important effect on the degradation of organic matter by UV-activated persulfate system. As shown in Fig. 8, as the concentration of transition metal ions (Cu^{2+}, Zn^{2+}, Co^{2+}) in the UV/PS system increased from 0 to 100 μM, k_{exp} increased from 1.96×10^{-3} to 2.44×10^{-3}, 3.11×10^{-3}, 2.62×10^{-3} s^{-1}, respectively. The results showed that the presence of transition metal ions can significantly promote the degradation of TMP. Take Co^{2+} for example, The main reason was that transition metal ions can activate PS to produce more $SO_4^{\bullet-}$, such as Eq. (12) (Liu et al. 2012; Nfodzo and Choi 2011).

$$M^{n+} + S_2O_8^{2-} \rightarrow M^{(n+1)+} + SO_4^{\bullet-} + SO_4^{2-} \qquad (12)$$

At the same time, the generated $M^{(n+1)+}$ is not stable, and $M^{(n+1)+}$ oxidative degradation of TMP may be another main reason for the significant increase in k_{exp} (Liang et al. 2013).

However, as the concentration of transition metal ions (Cu^{2+}, Zn^{2+}, Co^{2+}) in the system continued to increase from 100 to 400 μM, k_{exp} did not continue to increase but gradually decreased. The main reason was that excess transition metal ions can be combined with $SO_4^{\bullet-}$ to continue the reaction and consume free radicals (Eq. 24) (Furman et al. 2010; Nfodzo and Choi 2011), and excessive transition metal ions can also form hydrated ions with water (such as $[Zn(H_2O)_6]^{2+}$) as UV contenders affected TMP and $S_2O_8^{2-}$ absorption of UV.

$$M^{n+} + SO_4^{\bullet-} \rightarrow M^{(n+1)+} + SO_4^{2-} \qquad (13)$$

Transition metal ions showed a good synergistic effect in the UV/PS system. Only a very small amount of transition metal ions can significantly accelerate the degradation of organic pollutants, which provided a meaningful exploration for
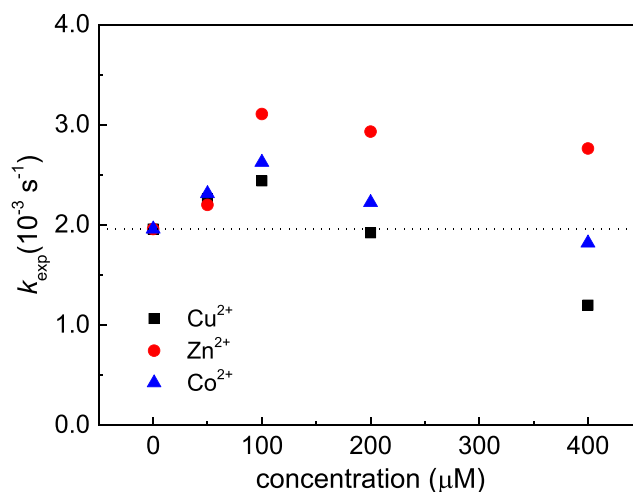

Fig. 8 Impacts of transition metal ions on the pseudo first-order constants of TMP (k) ($[TMP]_0 = 10$ μM, $[PS]_0 = 100$ μM, pH = 7.55, and $E_0 = 4.556 \times 10^{-6}$ Einstein L^{-1} s^{-1}).

the collaborative and comprehensive treatment of industrial wastewater.

Conclusions

The lower molar absorption coefficient and quantum yield limited the direct photolysis of TMP. After adding H_2O_2 or PS to the reaction system, the degradation effect of TMP was significantly enhanced, among which free radicals played a major role. $k_{HO^{\bullet},TMP}$ and $k_{SO_4^-,TMP}$ showed good agreement with previously reported values, which was measured by competitive kinetics method and steady-state assumption model. Steady-state approximation and kinetic model were also developed in order to predict and simulate the destruction of TMP by a variety of water matrices in UV-activated persulfate system. k_{obs} of TMP degradation decreased in the presence of FA and Cl⁻, but k_{obs} was increased with the concentration of PS. Transition metal ions had a good synergistic effect in UV/ PS degradation of TMP. However, excessive transition metal ions could reduce the TMP degradation due to the trapping effect of free radicals and the competition of formed hydrated ions against UV. The reported $k_{HO^{\bullet},TMP}$ and $k_{SO_4^-,TMP}$ values and effect of matrix components are more beneficial to predict and explain TMP degradation mechanism and select more efficient radical-based advanced oxidation processes in engineered water.

Declarations

Ethical approval Not applicable.

Consent to participate Not applicable.

Consent to publish Not applicable.

Competing interest The authors declare no competing interests.

References

Adams C, Wang Y, Loftin K, Meyer M (2002) Removal of antibiotics from surface and distilled water in conventional water treatment processes. J Environ Eng 128(3):253–260

Avetta P, Pensato A, Minella M, Malandrino M, Maurino V, Minero C, Hanna K, Vione D (2015) Activation of persulfate by irradiated magnetite: implications for the degradation of phenol under heterogeneous photo-fenton-like conditions. Environ Sci Technol 49(2): 1043–1050

Baeza C, Knappe DR (2011) Transformation kinetics of biochemically active compounds in low-pressure UV photolysis and UV/H_2O_2 advanced oxidation processes. Water Res 45(15):4531–4543

Beitz T, Bechmann W, Mitzner R (1998) Investigations of reactions of selected azaarenes with radicals in water. 2. chlorine and bromine radicals. J Phys Chem A 102(34):6766–6771

Beltran FJ, Ovejero G, Garcia-Araya JF, Rivas J (1995) Oxidation of polynuclear aromatic hydrocarbons in water. 2. UV radiation and ozonation in the presence of UV radiation. Ind Eng Chem Res 34(5): 1607–1615

Bougdour N, Tiskatine R, Bakas I, Assabbane A (2020) Textile wastewater treatment by peroxydisulfate/Fe(II)/UV: operating cost evaluation and phytotoxicity studies. Chemistry Africa 3(1):153–160

Bu Q, Wang B, Huang J, Deng S, Yu G (2013) Pharmaceuticals and personal care products in the aquatic environment in China: a review. J Hazard Mater 262(Supplement C):189–211

Buxton GV, Greenstock CL, Helman WP, Ross AB (1988) Critical review of rate constants for reactions of hydrated electrons, hydrogen atoms and hydroxyl radicals (·OH/·O⁻) in aqueous solution. J Phys Chem Ref Data 17(2):513–886

Criquet J, Leitner NKV (2009) Degradation of acetic acid with sulfate radical generated by persulfate ions photolysis. Chemosphere 77(2): 194–200

Das TN (2001) Reactivity and role of $SO_5^{\bullet-}$ radical in aqueous medium chain oxidation of sulfite to sulfate and atmospheric sulfuric acid generation. J Phys Chem A 105(40):9142–9155

Dong MM, Rosario-Ortiz FL (2012) Photochemical formation of hydroxyl radical from effluent organic matter. Environ Sci Technol 46(7): 3788–3794

Fang J-Y, Shang C (2012) Bromate formation from bromide oxidation by the UV/persulfate process. Environ Sci Technol 46(16):8976–8983

Fang GD, Dionysiou DD, Wang Y, Al-Abed SR, Zhou DM (2012) Sulfate radical-based degradation of polychlorinated biphenyls: effects of chloride ion and reaction kinetics. J Hazard Mater 227-228: 394–401

Fu J, Ji M, Wang Z, Jin L, An D (2006) A new submerged membrane photocatalysis reactor (SMPR) for fulvic acid removal using a nano-structured photocatalyst. J Hazard Mater 131(1):238–242

Furman OS, Teel AL, Watts RJ (2010) Mechanism of base activation of persulfate. Environ Sci Technol 44(16):6423–6428

Ghauch A, Baalbaki A, Amasha M, El Asmar R, Tantawi O (2017) Contribution of persulfate in UV-254nm activated systems for complete degradation of chloramphenicol antibiotic in water. Chem Eng J 317:1012–1025

Giannakis S, Lin K-YA, Ghanbari F (2021) A review of the recent advances on the treatment of industrial wastewaters by sulfate radical-based advanced oxidation processes (SR-AOPs). Chem Eng J 406: 127083

Grebel JE, Pignatello JJ, Mitch WA (2010) Effect of halide ions and carbonates on organic contaminant degradation by hydroxyl radical-based advanced oxidation processes in saline waters. Environ Sci Technol 44(17):6822–6828

Hou S, Ling L, Dionysiou DD, Wang Y, Huang J, Guo K, Li X, Fang J (2018) Chlorate formation mechanism in the presence of sulfate radical, chloride, bromide and natural organic matter. Environ Sci Technol 52(11):6317–6325

Huang Y, Kong M, Coffin S, Cochran K, Westerman D, Schlenk D, Richardson S, Lei L, Dionysiou D (2020) Degradation of contaminants of emerging concern by UV/H_2O_2 for water reuse: kinetics, mechanisms, and cytotoxicity analysis. Water Res 174:115587

Jayson G, Parsons B, Swallow AJ (1973) Some simple, highly reactive, inorganic chlorine derivatives in aqueous solution. Their formation using pulses of radiation and their role in the mechanism of the fricke dosimeter. J Chem Soc Faraday T 69:1597–1607

Ji Y, Zeng C, Ferronato C, Chovelon J-M, Yang X (2012) Nitrate-induced photodegradation of atenolol in aqueous solution: kinetics, toxicity and degradation pathways. Chemosphere 88(5):644–649

Ji Y, Xie W, Fan Y, Shi Y, Kong D, Lu J (2016) Degradation of trimethoprim by thermo-activated persulfate oxidation: reaction kinetics and transformation mechanisms. Chem Eng J 286:16–24

Ji Y, Yang Y, Zhou L, Wang L, Lu J, Ferronato C, Chovelon J-M (2018) Photodegradation of sulfasalazine and its human metabolites in water by UV and UV/peroxydisulfate processes. Water Res 133:299–309

Keen OS, Love NG, Linden KG (2012) The role of effluent nitrate in trace organic chemical oxidation during UV disinfection. Water Res 46(16):5224–5234

Kläning UK, Wolff T (1985) Laser flash photolysis of HClO, ClO⁻, HBrO, and BrO⁻ in aqueous solution. Reactions of Cl⁻ and Br⁻ atoms. Ber Bunsenges Phys Chem 89(3):243–245

Klaning UK, Sehested K, Appelman EH (1991) Laser flash photolysis and pulse radiolysis of aqueous solutions of the fluoroxysulfate ion, SO_4F. Inorg Chem 30(18):3582–3584

Kwon M, Kim S, Yoon Y, Jung Y, Hwang T, Lee J, Kang J (2015) Comparative evaluation of ibuprofen removal by UV/H_2O_2 and UV/$S_2O_8^{2-}$ processes for wastewater treatment. Chem Eng J 269:379–390

Lian L, Yao B, Hou S, Fang J, Yan S, Song W (2017) Kinetic study of hydroxyl and sulfate radical-mediated oxidation of pharmaceuticals in wastewater effluents. Environ Sci Technol 51(5):2954–2962

Liang Cj, Wang ZS, Mohanty N (2006) Influences of carbonate and chloride ions on persulfate oxidation of trichloroethylene at 20 °C. Sci Total Environ 370(2-3):271–277

Liang Hy, Zhang Yq, Huang Sb, Hussain I (2013) Oxidative degradation of p-chloroaniline by copper oxidate activated persulfate. Chem Eng J 218:384–391

Lin H, Ai J, Li R, Deng L, Tan W, Ye Z, Wu X, Zhang H (2020) Treatment of organosilicon wastewater by UV-based advanced oxidation processes: performance comparison and fluorescence parallel factor analysis. Chem Eng J 380:122536

Liu CS, Shih K, Sun CX, Wang F (2012) Oxidative degradation of propachlor by ferrous and copper ion activated persulfate. Sci Total Environ 416:507–512

Luo C, Jiang J, Ma J, Pang S, Liu Y, Song Y, Guan C, Li J, Jin Y, Wu D (2016a) Oxidation of the odorous compound 2,4,6-trichloroanisole by UV activated persulfate: kinetics, products, and pathways. Water Res 96:12–21

Luo CW, Jiang J, Ma J, Pang SY, Liu YZ, Song Y, Guan CT, Li J, Jin YX, Wu DJ (2016b) Oxidation of the odorous compound 2,4,6-trichloroanisole by UV activated persulfate: kinetics, products, and pathways. Water Res 96:12–21

Lutze HV, Bircher S, Rapp I, Kerlin N, Bakkour R, Geisler M, von Sonntag C, Schmidt TC (2015) Degradation of chlorotriazine pesticides by sulfate radicals and the influence of organic matter. Environ Sci Technol 49(3):1673–1680

McElroy WJ (1990) A laser photolysis study of the reaction of SO_4^- with Cl⁻ and the subsequent decay of Cl_2^- in aqueous solution. J Phys Chem 94(6):2434–2441

Naim S, Ghauch A (2016) Ranitidine abatement in chemically activated persulfate systems: assessment of industrial iron waste for sustainable applications. Chem Eng J 288:276–288

Neta P, Madhavan V, Zemel H, Fessenden RW (1977) Rate constants and mechanism of reaction of sulfate radical anion with aromatic compounds. J Am Chem Soc 99(1):163–164

Nfodzo P, Choi H (2011) Triclosan decomposition by sulfate radicals: effects of oxidant and metal doses. Chem Eng J 174(2):629–634

Nikravesh B, Shomalnasab A, Nayyer A, Aghababaei N, Zarebi R, Ghanbari F (2020) UV/Chlorine process for dye degradation in aqueous solution: mechanism, affecting factors and toxicity evaluation for textile wastewater. Journal of Environmental Chemical Engineering 8(5):104244

Parker CA, 1953 A new sensitive chemical actinometer. I. Some trials with potassium ferrioxalate. Proceedings of the Royal Society A 220 (1140), 104-116

Pereira VJ, Weinberg HS, Linden KG, Singer PC (2007) UV degradation kinetics and modeling of pharmaceutical compounds in laboratory grade and surface water via direct and indirect photolysis at 254 nm. Environ Sci Technol 41(5):1682–1688

Ran G, Li Q (2020) Degradation of refractory organic compounds from dinitrodiazophenol containing industrial wastewater through UV/H2O2 and UV/PS processes. Environ Sci Pollut R 27(6):6042–6051

Shah NS, He X, Khan HM, Khan JA, O'Shea KE, Boccelli DL, Dionysiou DD (2013) Efficient removal of endosulfan from aqueous solution by UV-C/peroxides: a comparative study. J Hazard Mater 263(Part 2):584–592

Stumm W, Morgan J (1996) Aquatic chemistry: chemical equilibria and rates in natural waters. Wiley, New York

Su R, Chai L, Tang C, Li B, Yang Z (2018) Comparison of the degradation of molecular and ionic ibuprofen in a UV/H_2O_2 system. Water Sci Technol 77(9):2174–2183

Sui Q, Wang B, Zhao W, Huang J, Yu G, Deng S, Qiu Z, Lu S (2012) Identification of priority pharmaceuticals in the water environment of China. Chemosphere 89(3):280–286

Tang T, Lu G, Wang R, Qiu Z, Huang K, Lian W, Tao X, Dang Z, Yin H (2019) Rate constants for the reaction of hydroxyl and sulfate radicals with organophosphorus esters (OPEs) determined by competition method. Ecotox Environ Safe 170:300–305

Vione D, Falletti G, Maurino V, Minero C, Pelizzetti E, Malandrino M, Ajassa R, Olariu R-I, Arsene C (2006) Sources and sinks of hydroxyl radicals upon irradiation of natural water samples. Environ Sci Technol 40(12):3775–3781

Wan Y, Xie P, Wang Z, Ding J, Wang J, Wang S, Wiesner MR (2019) Comparative study on the pretreatment of algae-laden water by UV/persulfate, UV/chlorine, and UV/H_2O_2: variation of characteristics and alleviation of ultrafiltration membrane fouling. Water Res 158:213–226

Wei Z, Villamena FA, Weavers LK (2017) Kinetics and mechanism of ultrasonic activation of persulfate: an in situ EPR spin trapping study. Environ Sci Technol 51(6):3410–3417

Weishaar JL, Aiken GR, Bergamaschi BA, Fram MS, Fujii R, Mopper K (2003) Evaluation of specific ultraviolet absorbance as an indicator of the chemical composition and reactivity of dissolved organic carbon. Environ Sci Technol 37(20):4702–4708

Xiao Yj, Fan Rl, Zhang Lf, Yue Jq, Webster RD, Lim TT (2014) Photodegradation of iodinated trihalomethanes in aqueous solution by UV 254 irradiation. Water Res 49:275–285

Xie PC, Ma J, Liu W, Zou J, Yue SYC, Li X, Wiesner MR, Fang JY (2015) Removal of 2-MIB and geosmin using UV/persulfate: contributions of hydroxyl and sulfate radicals. Water Res 69:223–233

Yang Y, Pignatello JJ, Ma J, Mitch WA (2014) Comparison of halide impacts on the efficiency of contaminant degradation by sulfate and hydroxyl radical-based advanced oxidation processes (AOPs). Environ Sci Technol 48(4):2344–2351

Yang Y, Pignatello JJ, Ma J, Mitch WA (2016) Effect of matrix components on UV/H_2O_2 and UV/$S_2O_8^{2-}$ advanced oxidation processes for trace organic degradation in reverse osmosis brines from municipal wastewater reuse facilities. Water Res 89:192–200

Yang ZH, Su RK, Luo S, Spinney R, Cai MQ, Xiao RY, Wei ZS (2017) Comparison of the reactivity of ibuprofen with sulfate and hydroxyl radicals: an experimental and theoretical study. Sci Total Environ: 590-591–751-760

Yu XY, Bao ZC, Barker JR (2004) Free radical reactions involving $Cl^•$, $Cl_2^{•-}$, and $SO_4^{•-}$ in the 248 nm photolysis of aqueous solutions containing $S_2O_8^{2-}$ and Cl. J Phys Chem A 108(2):295–308

Yuan F, Hu C, Hu Xx, Qu Jh, Yang M (2009) Degradation of selected pharmaceuticals in aqueous solution with UV and UV/H_2O_2. Water Res 43(6):1766–1774

Yuan R, Ramjaun SN, Wang Z, Liu J (2011) Effects of chloride ion on degradation of Acid Orange 7 by sulfate radical-based advanced oxidation process: implications for formation of chlorinated aromatic compounds. J Hazard Mater 196:173–179

Zhang R, Sun P, Boyer TH, Zhao L, Huang C-H (2015) Degradation of pharmaceuticals and metabolite in synthetic human urine by UV, UV/H_2O_2, and UV/PDS. Environ Sci Technol 49(5):3056–3066

Zhang B, Wang X, Fang Z, Wang S, Shan C, Wei S, Pan B (2021) Unravelling molecular transformation of dissolved effluent organic matter in UV/H_2O_2, UV/persulfate, and UV/chlorine processes based on FT-ICR-MS analysis. Water Res 199:117158–117158

Zhao R, Feng J, Liu J, Fu W, Li X, Li B (2019) Deciphering of microbial community and antibiotic resistance genes in activated sludge reactors under high selective pressure of different antibiotics. Water Res 151:388–402

Zuo Z, Cai Z, Katsumura Y, Chitose N, Muroya Y (1999) Reinvestigation of the acid–base equilibrium of the (bi) carbonate radical and pH dependence of its reactivity with inorganic reactants. Radiat Phys Chem 55(1):15–23